



Li Zhe (Orcid ID: 0000-0003-1743-7906)
Lu Lunhui (Orcid ID: 0000-0003-0507-0457)
Zhang Zengyu (Orcid ID: 0000-0002-2159-9329)

Imbalanced stoichiometric reservoir sedimentation regulates methane accumulation in China's Three Gorges Reservoir

Zhe Li¹, Lunhui Lu^{*1}, Pingyu Lv², Zengyu Zhang³, Jinsong Guo⁴

¹ CAS Key Lab of Reservoir Environment, Chongqing Institute of Green and Intelligent Technology, Chinese Academy of Sciences.

Address: No. 266 Fangzheng Avenue, Shuitu Hi-tech Industrial Park, Beibei, Chongqing 400714, China.

² Water-Environment Monitoring Center for the upper reach of Yangtze River, Chongqing, China.

Address: No. 410, Haier Road, Jiangbei District, Chongqing, 400021

³ Civil and Environmental Engineering, Technion – Israel Institute of Technology, Israel.

Address: Civil and Environmental Engineering, Technion – Israel Institute of Technology, Haifa 32000, Israel.

⁴ College of Environment and Ecology, Chongqing University, China.

Address: No. 174, Shazhengjie St., Shapingba District, Chongqing, 400044, China.

*Corresponding author: Lunhui LU (lulunhui@cigit.ac.cn)

Key Points:

- The mid-part of the Three Gorges Reservoir received bulk deposition of upstream sediments and was "control point" of methane accumulation.
- The longitudinal gradients of sediment stoichiometry and stable isotope reflect a shift of POM sources in mid-part of the reservoir.

This article has been accepted for publication and undergone full peer review but has not been through the copyediting, typesetting, pagination and proofreading process which may lead to differences between this version and the Version of Record. Please cite this article as doi: 10.1029/2019WR026447

- Sedimentation of particulate P was likely the potential key driver that drove particulate C:N:P in sediment, and regulated CH₄ accumulation.

Abstract

The river-reservoir continuum drives a separation of sedimentation along the longitudinal hydrodynamic gradients, potentially causing imbalanced stoichiometric sedimentation. However, there are still uncertainties regarding the contribution of imbalanced stoichiometric sedimentation to methane emissions along this continuum. A two-year field survey and in situ experiments were conducted in China's Three Gorges Reservoir (TGR), a river-valley dammed reservoir. Sediments were trapped and collected to analyze for particulate carbon (C), nitrogen (N) and phosphorus (P) concentrations of different sizes in the summer flooded and winter dry seasons along the main stem. Large amount of sediments were deposited in the mid-part of the TGR, particularly in the summer flood season. Hydrodynamic gradients structured imbalanced stoichiometric sedimentation patterns. Averaged particulate C:N:P proportions in the sediment layer along the upper, mid and lower part of the TGR in the first 30 years of reservoir operation were estimated to be 68:7:1, 97:8:1, 151:13:1 respectively. The mid-part of the TGR, being the "control point" of methane accumulation based on seasons, exhibited the shift in stoichiometry and the stable isotope signatures indicating that there was likely a shift in sources of POM. P, specifically in smaller size particles (<10 μm), seemed to be the potential key driver that regulates particulate C:N:P in the sediment of the TGR. Its sedimentation, primarily in the mid-part of the TGR, contributed to the significant decreases in particulate C/P ratios, and could possibly regulate long-term CH₄ accumulation in the reservoir.

Key words: sedimentation rate, river-reservoir continuum, organic carbon, size of sediments, greenhouse gas

1 Introduction

Lakes and reservoirs are significant regulators of greenhouse gases (GHG), such as methane (CH₄) and carbon dioxide (CO₂) [Tranvik *et al.*, 2009; Williamson *et al.*, 2009]. Excessive carbon (CO₂+CH₄) emissions from reservoirs have attracted global concern for the last two decades [Barros *et al.*, 2011; Cole *et al.*, 2007; Tranvik *et al.*, 2009], not only because of their importance to carbon cycling through the "freshwater pipe" [Cole *et al.*, 2007; Deemer *et al.*, 2016] but also because the global hydropower industry needs to clarify its carbon footprints and credits for trade in the new era of global change under the Paris Agreement [Hertwich, 2013; Z Li *et al.*, 2017a]. It has been widely agreed that excessive carbon (C) emissions are caused mainly by decomposition or degradation of flooded organic matter (OM) in either oxic or anoxic conditions due to changes in hydro-morphological and physio-chemical conditions caused by reservoir impoundment and operation [Prairie *et al.*, 2018]. While degradation of OM in reservoirs tends to show a long-term exponential decay [Abril *et al.*, 2005; Robert Delmas *et al.*, 2005], reservoir C emissions are at their peak during the first several years after impoundment and gradually decrease to a level which is comparable to similar natural lakes after 15 to 20 years. Hence, reservoir age is regarded as an important variable that could be used to predict long-term GHG emissions [Abril *et al.*, 2005; Barros *et al.*, 2011; R. Delmas *et al.*, 2001].

In general, macroelements, such as nitrogen (N) and phosphorus (P), organic matter (OM), terminal electron acceptors (TEAs), and temperature are defined as proximate controls due to their direct involvement in biochemical processes of CH₄ generation [Stanley *et al.*,

2016]. CH₄-generating habitats in reservoirs share a common trait of having ample stocks of OM that provide the fuel for respiration and allow CH₄ production in an anoxic and highly reducing environment to progress to the point when methanogenesis is the only remaining option [Stanley *et al.*, 2016]. Change of hydrological and geomorphological characteristics in a reservoir affect the above proximate controls regulating methane production. Damming has caused bulk sedimentation and burial of organic carbon (OC) in reservoirs. Sedimentation of reactive OC could also stimulate the formation of anoxia in the sediment layer and/or DO stratification by the consumption of limited dissolved oxygen [Sobek *et al.*, 2012]. A positive correlation between sedimentation rates and methane production, supports the inference that reservoir sedimentation drove methane emissions from reservoir impoundments [A. Maeck *et al.*, 2014; A Maeck *et al.*, 2013]. Particularly, littoral shallower water areas of reservoirs receive highly methanogenic sediments and are the most productive areas for methane [Peeters *et al.*, 2019], mostly in ebullient forms [Powers *et al.*, 2013; Stanley *et al.*, 2016], making the areas as an OC sink but methane source [Sobek *et al.*, 2012]. Thus, reservoirs could exhibit long-term methane production and emission if continuously received upstream OC input and sedimentation. Reservoir age, as a potential measure of flooded and decomposed OM, may not be the only parameter to estimate long-term trends of reservoir methane production and emission.

Nevertheless, there are still uncertainties regarding the contribution of reservoir sedimentation to C emissions. Suspended riverine sediments are mainly derived from different OM sources, e.g., biological fragments, and aquatic detritus, mixed or associated with inorganic minerals in the form of flocs or aggregates. When transported from rivers into reservoirs, sedimentation separation occurs along the river-reservoir gradient due to density differences and changes in hydrodynamic conditions. Heavier inorganic minerals tend to be among the first to settle, whereas organic sediments are likely to be transported further because they are of lower density. It is still not well reported whether this sedimentation separation exerts effects on C emissions along the river-reservoir gradient. Sedimentation along the river-reservoir gradient may also cause stoichiometric imbalance in reservoir sediments [Grantz *et al.*, 2014]. Since methane production strongly depends upon the stoichiometry of OM, e.g., the C:N ratio, as an indicator of bioavailability for methanogenic microorganisms [Grasset *et al.*, 2018], it can be inferred that imbalanced stoichiometric sediments caused by sedimentation separation along the river-reservoir gradient might potentially drive the methane balance. The above questions are important for global methane cycling and for reservoir operations in the context of the life cycle of reservoir carbon management for mitigating methane production and emissions, yet there is lack of information and further research is needed.

A two-year field survey and in situ sedimentation trap experiments were carried out along the 660 km river-reservoir gradient in China's Three Gorges Reservoir (TGR) in 2014 and 2015. Particulate C, N and P were trapped both in the summer flooded season and in the winter dry season and were separated into different sizes from a set of sampling sites along the river-reservoir continuum. In the study, we attempted to show the evidence that dissolved CH₄ will vary with sediment stoichiometry through synthetic observations and modeling analysis. The aim of our study is to explain how the imbalanced stoichiometry of reservoir sediments regulates the dissolved CH₄ in the river-valley dammed reservoir.

2 Materials and Methods

2.1 Site description and sampling summary

The Three Gorges Reservoir (TGR) is a subtropical river valley dammed reservoir. Creation and impoundment of the reservoir affected about 700 km of river reach of the main stem of the Yangtze and involved 632 km² of flooded land. Constrained by the Yangtze river valley, the ratio of length to width of the TGR is 650:1. The full reservoir capacity is 39.3 km³. The water surface area of the TGR at its normal water level (175 m above the sea level) was 1,084 km², which is only 1.5 times larger than the water surface of the affected river reach.

Initial impoundment of the TGR started in 2003 and continued to 2010 when its water level reached to 175 m for the first time. Serving mainly for flood control and hydropower production, the TGR undergoes large seasonal water level fluctuations. The water level of the TGR is drawn down to 145 m in May before the summer flood season, preparing 22.1 km³ of volume for storing possible floods and releasing accumulated bottom sediments. In September and October of each year, after the flood season, the water level of the TGR increases to 175 m to maximize its function of hydropower production. During the spring and early summer (from February to May), the TGR gradually increases its downstream discharge and lowers its water level from 175m to 145m to maintain acceptable flow condition for downstream fish spawning, and to meet the needs for downstream navigation and water supply. This operation scheme significantly amplifies the variations of water retention time in a yearly cycle. In summer, the water retention time of the TGR is mostly less than 20 d, whereas the water retention time in winter is approximately 80 d. Shifts in water retention time significantly structured the distinctive aquatic ecosystem between a mostly lotic type in summer and a nearly lentic type in winter in the TGR [Z Li *et al.*, 2017b; Xiao *et al.*, 2016]. These hydro-morphological characteristics supports our experimental design for an in-situ sediment trapping experiment in these two seasons.

Seven sampling sites were selected in the main stem of the Yangtze in the TGR (Figure 1). ZT was the reference site that was not impacted by flooding and operation of the reservoir. All the other sampling sites could be expressed by the distance downstream from ZT (Table 1). Thus, the whole reservoir along the Yangtze main stem could be then divided into three sections (Figure 1). The upper part of the reservoir was approximately from 0 km to 250 km, covering ZT and CT sampling sites. The mid part of the TGR was from 250 km to 500km, covering FL, ZX and WZ sampling sites. The lower part of the reservoir was from 500 km to the dam site, approximately 732 km downstream of ZT.

Table 1 List of sampling sites and their locations in the reservoir

	Site names	Coordinate	Downstream distance from ZT (km)
Upper part	ZT	29°00.796'N, 105°51.170'E	0
	CT	29°35.858'N, 106°37.58'E	139
Mid-part	FL	29°47.535'N, 107°27.738'E	254
	ZX	30°25.194'N, 108°10.615'E	356
	WZ	30°42.144'N, 108°23.235'E	445
Lower part	FJ	31°02.600'N, 109°31.855'E	568
	ZG	30°51.217'N, 110°58.502'E	730

In situ sediment trapping experiments were carried out both in August and November, corresponding to the summer flood season and winter dry season. Cylindrical polymethyl sediment traps were 90 cm in height with diameters of 7 cm. Three sediment traps were fixed and sealed by two horizontal plastic plates, grouped into a parallel set and deployed onsite for one week at each sampling site (Supporting information S1). At each sampling site, sediment

traps were deployed at the surface (1.5 m below the water surface) and in the middle and bottom layers (5 m above the bottom of the main stem) in the water column. A unique roping system in combination with a 10 kg-20 kg iron plummet at the bottom of each set was adopted to keep the sets of sediment traps vertical and resistant to water velocity and turbulence. Specifically, for the upper 260 km river reach in the TGR, i.e. river reach from ZT to FL, it was assumed that the water column was completely mixed during the summer flood season. The sets of sediment traps in these three sampling sites were only deployed in the upper layer of the water column (1.5 m under water surface). In the winter high water level period, additional bottom layers of sediment traps were deployed in CT (139 km) and FL (254 km) but not in ZT (0 km). When deploying the sets of sediment traps, suspended sediments at the same layer were simultaneously sampled as references for the collected samples.

Five-liter (5 L) water samples were collected at various depths at the same time as sediment trap deployment. These depths were 0.5 m, 5 m, 10 m, 20 m, and each additional 10 m (depending on the depth of water column) until 2.0m above the bottom of the main stem. Three-dimensional instant water velocity and detection of water column depth were measured onsite by using a Flow Quest® Flowsic 600 acoustic current profiler (Link Quest Inc., CA, USA). Profiles of temperature, dissolved oxygen (DO), pH and conductivity were measured using a calibrated YSI® Pro 2030 probe (YSI Inc., Ohio, USA). Additional profile measurements were performed when collecting the sediment traps.

Ebullition is an important pathway of CH₄ emission particularly in shallower waters [DelSontro et al., 2015; McGinnis et al., 2006; Walter et al., 2008; Wilkinson et al., 2019]. In the main stem of the TGR, water depth gradually increases from 8 ~ 15 m in the upper part to more than 100 m at the dam site. In the mid and lower part of the TGR, increased water depth (> 20 m and more) in the main stem restricts the formation of gas bubbles. Thus, ebullition was assumed to be negligible in mid and lower part of the TGR. However, higher turbulence and shear stress may still promote ebullition of methane [Aben et al., 2017; DelSontro et al., 2015; Sollberger et al., 2017]. This could be the case in the upper part of the TGR. Yet, we could not provide direct evidence to support the inference. Thus, in this study, we limited our discussion to the dissolved CH₄ in the TGR.

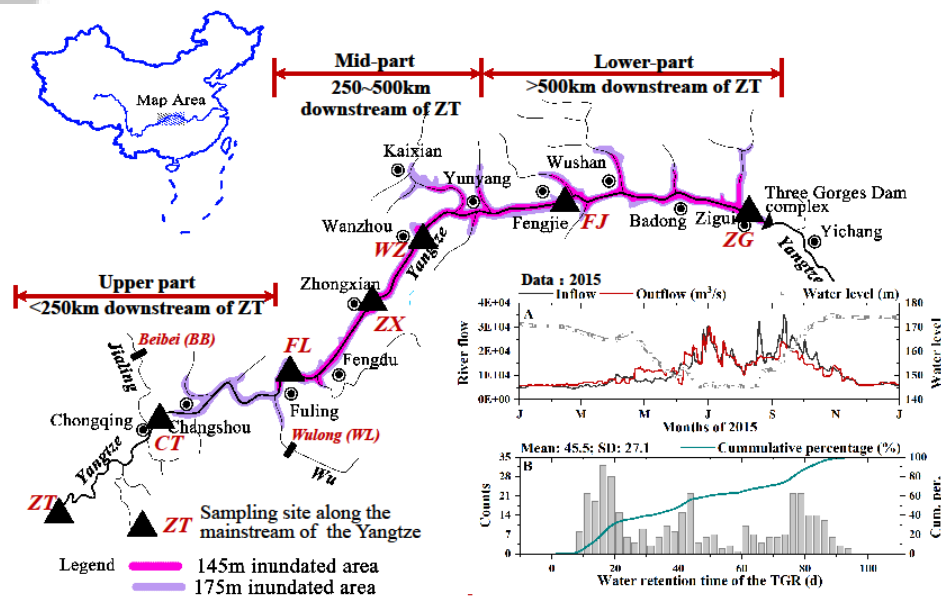


Figure 1 Sampling sites in the Three Gorges Reservoir. The right bottom panel A shows the daily inflow, outflow and water levels at the dam site of the TGR in 2015. Data were

accessed from the China Three Gorges Corporation (<http://www.ctg.com.cn>). Panel B shows the corresponding distributions of water retention times of the reservoir. Beibei (BB) and Wulong (WL) are respectively the background cross sections of the Jialing River and the Wu River, the two largest tributaries of the Yangtze in the TGR.

2.2 Measurements of CH₄, CO₂ and dissolved nutrients in water phase

The headspace approach was applied to measure the CH₄ and CO₂ concentrations at different depths in the water column. Measurement of the CH₄ and CO₂ concentrations in the water column followed the measurement guidelines proposed by the International Hydropower Association [Goldenfum, 2010]. In brief, 20 mL water samples were collected in triplicate in headspace bottles and were carefully sealed while under the water surface. Then, 5 mL highly-purified nitrogen gas was injected into the water samples to create a headspace followed by a 20 min shaking equilibrium. Gas samples were then analyzed for CH₄ and CO₂ using a gas chromatograph (Agilent® 7820A, USA) equipped with a 0.25-mL sampling loop, a steel packed TDX-01 column, a flame ionization detector and a methane reformer.

Water samples for chemical analysis were filtered through pretreated (combusted at 450°C for 4 h in a muffle furnace and weighed after cooling) Whatman® GF/F glass fiber membranes. The filtrates were used for analysis of dissolved organic carbon (DOC) by using a Shimadzu® TOC-V TOC analyzer (Shimadzu®, Japan). Dissolved total nitrogen (DTN) and total phosphorus (DTP) were analyzed by standard method according to [APHA *et al.*, 2005].

2.3 Physicochemical analysis of suspended and trapped sediments

In this study, total particulate matter (TPM) indicated all solids (or called as "sediments") in water samples that could not pass Whatman® GF/F glass fiber membranes. Thus, the terminology of TPM is used here to indicate the term "sediments". For simple expression, the terminology of "sediments" is more frequently used in the paper. "Suspended sediments" refers to the TPM in water column. Correspondingly, "trapped sediments" means the TPM trapped by our sediment traps. In addition, particulate organic matter (POM) refers to the total organic matter attached on the surfaces of inorganic sediment or as a whole or part of sediments. Concentration of POM is less than TPM in the TGR.

Concentrations of both TPM and POM could be estimated through weighed difference method. Three subsamples of field water samples with the same volume, normally 500 mL in summer and 1 L or more in winter, were passed through different sizes of Sefar® Nitex nylon mesh (Heiden, Switzerland), i.e., 50 µm, 30 µm, 10 µm. The filtrates were then filtered through pre-weighed GF/F filters. One subsample with the same volume was also directly filtered through a pre-weighed GF/F filter without any mesh filtration. All residues on the GF/F filters were dried at 65°C for 48 h-72 h and re-weighed. The TPM was the weighed difference between pre-weighed GF/F filter and the dry sediments divided by the volume of water filtered. Then, concentrations of TPM in different size ranges, e.g., <50 µm, <30 µm, and <10 µm was calculated. Their arithmetical differences were estimated as the TPM between different ranges, e.g., <10 µm, 10~30 µm, 30~50 µm, and >50 µm. After these weights, GF/F filter with dried fresh residues were subsequently combusted at 450°C for 4 h and weighed after cooling down to room temperature. The concentration of POM of difference sizes were the difference in mass before and after the combustion treatment divided by the volume of water filtered. The 65°C dried fresh residues were also used for elemental composition analysis of C, N and P. Triplicates were performed for quality control.

After a one-week collection period in summer (10 days in winter), water above the sediment layer in the traps was carefully pumped from the top of the traps down to the layer slightly above collected sediments by a small peristaltic pump on site to minimize disturbances. Volumes of collected sediment layers (slurry with water) were calculated from the height of the sediment layers and diameter of the trap. The collected sediments were then poured from the traps and transported into pre-weighed and dried plastic sample boxes. The traps were then rinsed with limited distilled water, and the volume of usage was recorded to adjust for the weight introduced by the slurry. Slurries with specific volumes were treated according to the same protocol discussed above for fractionation. Triplicates were applied for quality control. Mass collection efficiencies for this methodology are estimated to be $\geq 90\%$ [Baker *et al.*, 1991; Hamilton-taylor *et al.*, 1984; Meyers *et al.*, 1984].

Particulate organic carbon (POC), particulate organic nitrogen (PON), as well as $\delta^{13}\text{C}$ -POC and $\delta^{15}\text{N}$ -PON, were measured by a Thermo Fisher[®] Flash H T Elemental Analyzer for Isotope Ratio MS (Thermo Fisher Scientific, MA, USA). The standard reference materials were Vienna Pee Dee Belemnite for carbon and atmospheric N_2 for nitrogen. Acid extraction and the ammonium molybdate coulometric method were used for measurement of particulate phosphorus (PP), for which the detection limit is 0.0021 mgP/L. In winter, PP levels in both the suspended and trapped sediments were below the detection limit.

2.4 The SIAR Mixing Model

Relative contribution of variable sources of OM were estimated by using stable isotope mixing model "SIAR" (Stable Isotope Analysis in R) [A Parnell *et al.*, 2008]. The model SIAR is based on two main Bayesian statistical methods: a mixing model for estimating the proportional contribution of sources to a mixture; and quantitative tools for comparing dispersion in isotope-space [A C Parnell *et al.*, 2010]. The model SIAR includes the residual error term in the form of standard deviation. To estimate the contribution of POM sources, the endmembers values were compiled from publications in the Yangtze river [Wang *et al.*, 2014; Wu *et al.*, 2007]. In particular, endmember values of plankton, C3 and C4 plants were from Wang *et al.* [2014]. Endmember values of soil were selected from Wu *et al.* [2007].

Table 2. Endmembers values used in stable isotope analysis.

Endmembers (Mean \pm SD)	$\delta^{13}\text{C}$ -POC (‰)	$\delta^{15}\text{N}$ -PON (‰)
C3	-29.4 \pm 1.7	1.5 \pm 2.3
C4	-12.9 \pm 1.7	-0.8 \pm 4.3
soil	-26.1 \pm 0.3	3.3 \pm 1.3
Plankton	-24.6 \pm 2.3	3.9 \pm 2.4

2.5 Sediment modeling and prediction

A one-dimensional, nonuniform sediment model was applied to model the transport and deposition of different-sized sediments in the TGR. Modeling work was described in detail by Zhou and Lin [1998] and Zhou *et al.* [2015]. The entire TGR was defined with 432 cross sections as computational nodes from ZT to the dam site, including 756 km in the main stem, and 65 and 67 km in the tributary backwater areas of the Jialing and Wu Rivers, respectively. The nonuniform sediment was resolved using eight fractions with diameters of 1.9, 6.0, 16.4, 43.5, 87.0, 124, 198, and 368 μm , which were converted to 7.4, 16.9, 36.8, 62.0, 87.2, 124, 198, and 368 μm , respectively, to account for the effects of flocculation or aggregation in sediments [Xiang, 2000].

The measured 10-year flow series and sediment hydrographs from the upstream boundary at ZT, BB (the reference site of the Jialing River, Figure 1) and WL (the reference site of the Wu river, Figure 1) from 1961 to 1970 were used in the model for consistency with the design conditions for this project, representing the pristine runoff of water (449 Mm³/yr) and sediment (541 Mt/yr). Another 10-year measured series of inflow and sediment, i.e., from 1993 to 2002, with an average inflow of 429 Mm³/yr and sediment inflow of 345 Mt/yr were also used in the model, representing the nearest 10-year series prior to reservoir impoundment. The average size distributions, annual water, and sediment inputs to the TGR and the reservoir operation scheme were used in the model computations. Reservoir operations were based on the abovementioned operation scheme, as described in section 2.1.

The model was previously verified and validated by field data and applied to many case studies that specifically addressed reservoir sedimentation analysis and management after formation and operation of the reservoir in 2003. By recycling the series, the sedimentation processes were predicted for 30 years with a computational time step of 5 min [Zhou *et al.*, 2015]. It was assumed that adsorption and desorption between sediment and water were at equilibrium; thus, no boundary conditions for C, N and P were required [Zhou *et al.*, 2015].

Since POC, PON and PP significantly and positively correlated with the sedimentation rates of TPM (Supporting information S2), the burial of C, N and P in reservoir sediments was estimated based on their relative abundance in TPM from field data. Mineralization, respiration and denitrification of C and N might cause continuous losses of C and N from the reservoir sediment layer. However, we did not test burial rates of C and N directly onsite, which is a limitation of our study. We applied empirical data of OC burial efficiency, i.e., the ratio between buried and deposited OC, to estimate the OC in reservoir sediments after a long period [Clow *et al.*, 2015; Mendonca *et al.*, 2016]. OC burial efficiencies in the upper, mid and lower parts of the TGR were estimated to be 80%, 60%, and 45%, respectively [Mendonca *et al.*, 2016]. For nitrogen, we could not find any publication related to burial efficiencies of nitrogen in lakes or reservoirs, particularly in subtropical ones. The burial efficiency of nitrogen in the TGR was thus assumed to be the same as for OC in our long-term estimation.

2.6 Data analysis

Simultaneous hydrological data during our study period were directly downloaded from the website of China Three Gorges Corporation. These data included real-time water level of the TGR, as well as reservoir inflow and outflow. We averaged the real-time hydrological data into daily values. Data analyses (descriptive statistics, linear regression, One-way ANOVA and post hoc tests) were performed using OriginPro[®] 2018 (OriginLab Corporation, MA, USA). In One-way ANOVA, differences between means were considered significant at $p < 0.05$. The stable isotope model SIAR was implemented in the R program ([Team, 2020]).

3 Results

3.1 Reservoir sedimentation: rates and stoichiometry

Sedimentation of TPM in the TGR showed significant seasonal and longitudinal variations. Summer flood seasons received a majority of external sediments from upstream of the Yangtze, and its tributaries. The sedimentation rates of TPM and POM were 30 ~ 40 times higher than those in winter (Table 3). The mid-part of the TGR received the largest amount of sediments (Supporting information S1). The sedimentation rate of TPM at 139 km downstream of ZT in summer was 51,428.15 g/(m²·d), which is among the highest for all sampling sites. Towards downstream, the sedimentation rates for both TPM and POM decreased. The trapped

sediments consisted mostly of the large fraction size ($>50 \mu\text{m}$), making up 92% of the sediments at 139 km river reach (Supporting information S3). Medium-large particulates ($30 \sim 50 \mu\text{m}$) were also important contributors to the trapped sediments. Their contributions in the mid-part of the TGR were relatively higher compared with other sampling sites.

In trapped sediments, the ratio of POM/TPM were significantly lower than suspended sediments in large size of sediments ($>50 \mu\text{m}$, and $30 \sim 50 \mu\text{m}$), indicated that large-sized trapped sediments were much more inorganic than suspended sediments. With small size of sediments ($<10 \mu\text{m}$), such difference was not evident (Supporting information S4). In addition, sedimentation rate of C, N, and P strongly depended on the sedimentation rate of POM and TPM. They showed significant positive correlation (Supporting information S4).

DOC sampled in the summer across all sampling sites in the TGR ranged between 4.80 mg/L and 5.77 mg/L, with a mean value of 4.96 ± 0.17 mg/L (Mean \pm Standard Error). In winter, DOC increased to 5.97 ± 0.30 mg/L. The mean values of DTP and DTN in summer were 0.056 ± 0.005 mg/L, and 1.84 ± 0.07 mg/L respectively. In winter, the mean value of DTP and DTN in the TGR was 0.092 ± 0.006 mg/L, and 1.63 ± 0.03 mg/L respectively. Thus, mean value of DOC/DTN in terms of mole ratios in summer were 3.16 ± 0.07 . In winter, DOC/DTN mole ratio in the TGR was 4.28 ± 0.22 (Figure 2).

The stoichiometry of C, N and P in the trapped sediments differed from that in the suspended sediments. Trapped sediments had relatively higher C/N ratios in both the summer and winter seasons, and these were generally higher than the Redfield ratio [Redfield, 1960] (dashed lines in Figure 2A and 2B). In contrast, the stoichiometry of dissolved nutrients was lower than the Redfield ratio. This difference increased with increases in sediment size, despite the summer samples with sizes $>50 \mu\text{m}$. Both suspended and trapped sediments had significantly higher C/N ratios than the dissolved forms (Figure 2A). The N/P ratios in suspended sediments in the summer generally did not show significant differences between the trapped and suspended sediments (ANOVA, $p>0.05$), except for the N/P ratios in summer for the size ranges of $10 \sim 30 \mu\text{m}$ and $30 \sim 50 \mu\text{m}$ in which the trapped sediments had significantly lower N/P ratios. There were also no significant differences in C/P ratios between trapped sediments and suspended sediments (ANOVA, $p>0.05$). The dissolved C/P ratios were roughly the same for both types of sediments.

Accepted

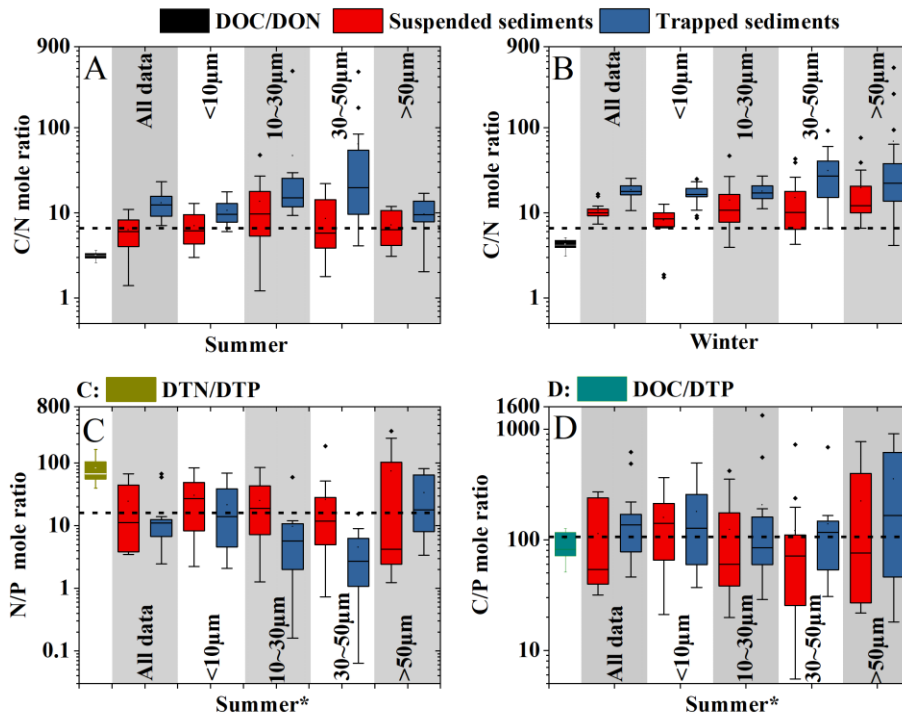


Figure 2 Differences in stoichiometry of suspended and trapped sediments in the study. A & B), the C/N ratios of suspended and trapped sediments for different sizes in summer and winter; C & D), the N/P and C/P ratios of suspended and trapped sediments for different sizes in summer. PP in winter samples were below the detection limit.

Table 3 Sedimentation rates of sediments for all sampling sites in the Three Gorges Reservoir (Unit: $\text{g}/(\text{m}^2 \cdot \text{d})$). Very few sediments were collected in the winter. Thus, particulate phosphorus (PP) were below the detection limit. PP data were not available in winter.

0	Summer		Winter	
	Mean \pm Std. V	Range	Mean \pm Std. V	Range
TPM	4,789.30 \pm 12,948.75	28.83-51,428.15	125.95 \pm 241.45	8.73-928.46
POM	355.19 \pm 1,013.42	2.58-4,008.4	11.11 \pm 19.87	1.26-71.40
POC	72.77 \pm 62.72	1.23~245.94	2.11 \pm 3.80	0.17~12.80
PON	6.86 \pm 5.69	0.16~18.43	0.11 \pm 0.17	0.01~0.58
PP	1.45 \pm 1.32	0.06~4.70	N/A	N/A

Heterogeneity of sediment compositions resulted in longitudinal stoichiometric variations downstream (Supporting information S5). Compared to the suspended sediments, the trapped sediments showed higher C/N and C/P ratios (Figure 3). Trapped sediments from the upstream sampling sites, e.g., ZT, CT and FL, showed relatively higher C/N ratios (above than the Redfield ratio) and lower C/P ratios (below than the Redfield ratio). In contrast, the

downstream sampling sites, e.g., FJ and ZG, exhibited relatively lower C/N ratios (below the Redfield ratio) and higher C/P ratios (higher than the Redfield ratio). In trapped sediments (Figure 3B), the C/N and C/P ratios were generally negatively correlated, despite of the largest size range (>50 μm). Stoichiometry of dissolved constituents did not show significant correlation (Spearman, $p>0.05$) with particulate forms in our datasets.

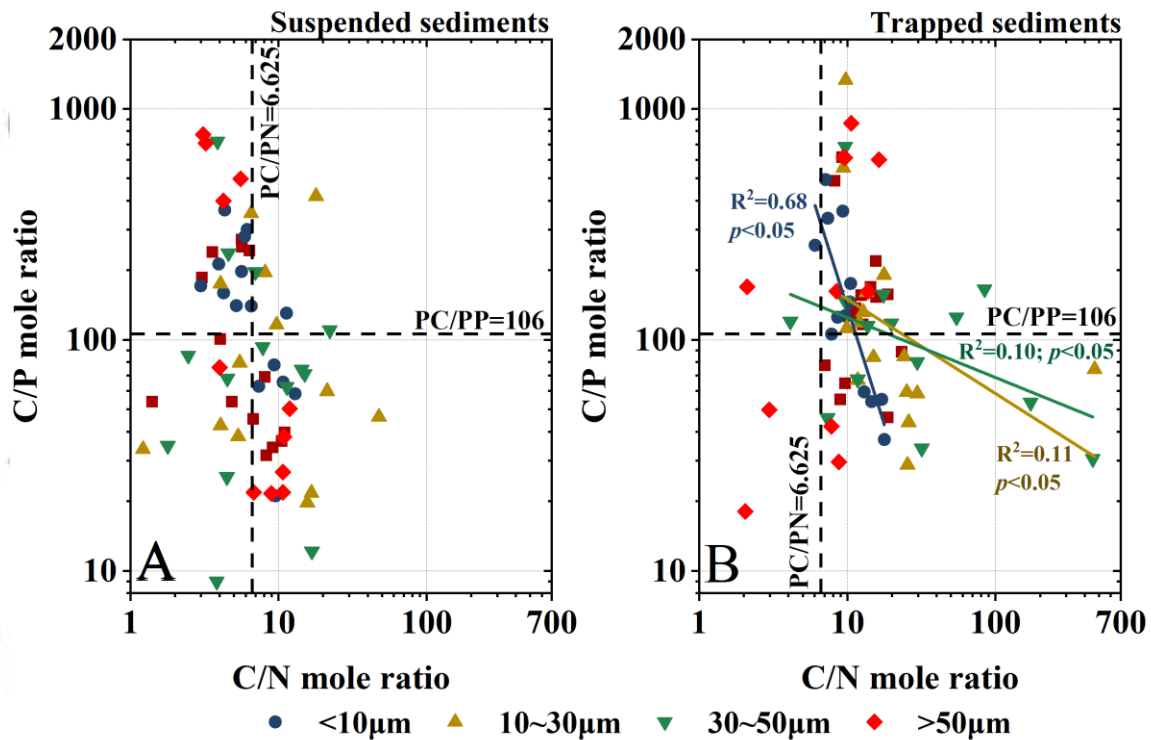


Figure 3 Scatter plots between particulate C/N mole ratio and particulate C/P mole ratio in both suspended sediments (A) and trapped sediment (B). In B, R^2 and p near the fitted lines with the same color illustrated the linear regression results. Vertical and horizontal dash lines in the both A and B were the references lines of Redfield ratios [Redfield, 1960].

3.2 Stable isotopic ratios of particulate carbon and nitrogen

$\delta^{13}\text{C}$ -POC in upper part of the TGR showed significant differences between summer and winter (Table 4). However, the downstream sampling sites did not show significant differences between the two distinctive seasons (Figure 4 A). Similarly, there were distinctive longitudinal trends for $\delta^{15}\text{N}$ -PON between the two seasons despite the values at the dam site (Figure 4 B). The stable isotopic ratios of POC and PON implied that the POM originated from different sources in the TGR. In summer, most OM in the trapped sediments may have been from terrestrial OM originating from C3 plants and soils, as most of the $\delta^{13}\text{C}$ -POC points were clustered within a range between -24‰ ~ -26‰ , and the C/N mole ratios were within a range of 5 ~ 10 (Figure 4 C). In the upper part of the reservoir, the higher $\delta^{13}\text{C}$ -POC ($> -20\text{‰}$) and C/N mole ratios (>3) indicated that the contributions from terrigenous OM (C4) were not negligible (Supporting information S6). Sampling sites in the lower part of the reservoir had relatively abundant autochthonous OM compared to the mid and upper parts of the TGR. In winter, the

extended water renewal time of the TGR created an environment that caused homogenization of OM in the TGR. Most of the trapped OM was mainly from mixture of C3 plants and soils, which may have originated from the reservoir drawdown area (Figure 4 D).

Table 4 Ranges of $\delta^{13}\text{C}$ -POC, $\delta^{15}\text{N}$ -PON in suspended and trapped sediments

Units: ‰			Mean	Range
Suspended Sediments	$\delta^{13}\text{C}$ -POC	Summer	-26.71 ± 0.43	-28.22~-25.12
		Winter	-24.50 ± 0.52	-27.43~-20.14
	$\delta^{15}\text{N}$ -PON	Summer	5.57 ± 1.15	-0.38~9.04
		Winter	6.98 ± 0.86	0.21~10.91
Trapped sediments	$\delta^{13}\text{C}$ -POC	Summer	-24.29 ± 0.85	-26.01~-17.20
		Winter	-25.01 ± 0.25	-25.81~-21.34
	$\delta^{15}\text{N}$ -PON	Summer	4.48 ± 0.82	-0.34~9.39
		Winter	5.02 ± 0.56	-0.20~7.97

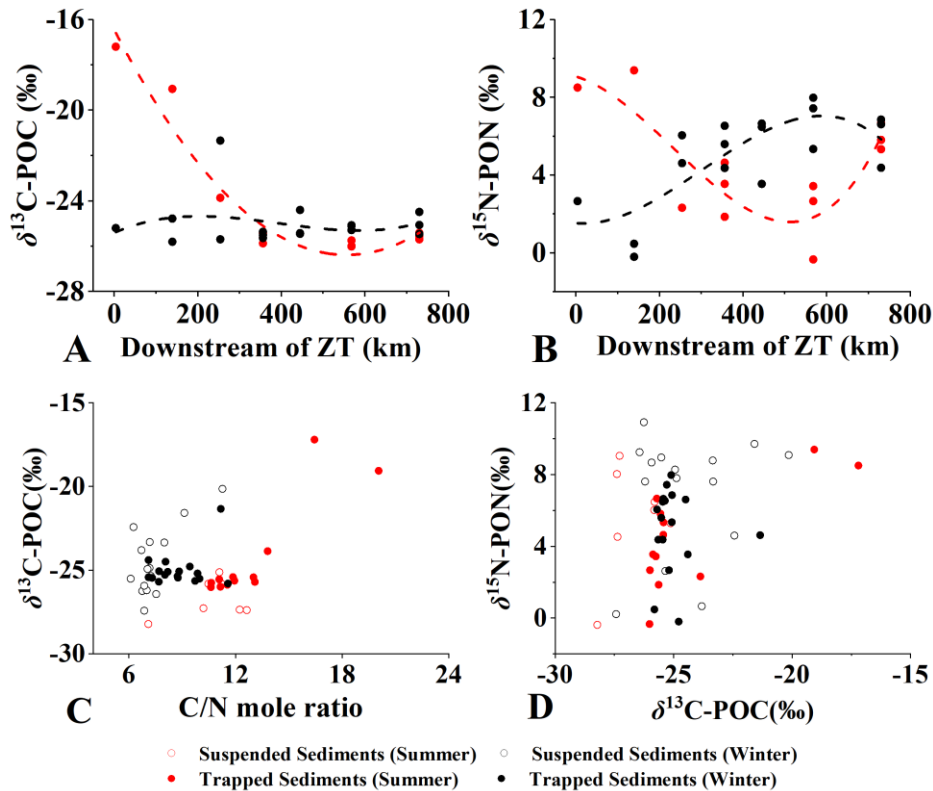


Figure 4 Stable isotopes of $\delta^{13}\text{C}$ -POC and $\delta^{15}\text{N}$ -PON in trapped and suspended sediments. A) & B) longitudinal gradients of $\delta^{13}\text{C}$ -POC and $\delta^{15}\text{N}$ -PON in trapped sediments in summer and winter. Dashed lines in both figures were smoothed curves. C), biplots of $\delta^{13}\text{C}$ -POC and C/N ratios. D) biplots of $\delta^{13}\text{C}$ -POC and $\delta^{15}\text{N}$ -PON.

3.3 Longitudinal profiles of CH₄ and other parameters.

Longitudinal profile of the CH₄ showed that the mid-reach was the "control point" of CH₄ in the TGR (Figure 5) [Bernhardt *et al.*, 2017]. On average, CH₄ concentration in both seasons was $0.441 \pm 0.117 \mu\text{mol/L}$ in the mid-part of the reservoir, approximately 1.7 times higher than the lower part of the reservoir. In winter, maximum CH₄ were found in the mid-part of the reservoir. The mean value of the CH₄ concentration at the 254km river reach was $0.611 \pm 0.128 \mu\text{mol/L}$, about five times greater than 568 km river reach ($0.111 \pm 0.057 \mu\text{mol/L}$). The lower part of the reservoir, 560 km to 650 km, had the lowest CH₄ concentration in water column in winter. In the summer flood season, CH₄ apparently accumulated at the bottom (>30 m under the water surface) in the mid-part of the TGR (Figure 5). Stratification of CH₄ at the lower part of the reservoir were evident in both seasons, which generally corresponded well to a vertical DO profile in the same area. At the dam site, surface CH₄ levels were $0.093 \pm 0.004 \mu\text{mol/L}$ on average, whereas the bottom CH₄ concentrations were approximately 3 times higher than that at the surface. CO₂ concentrations in the TGR seemed to be homogeneously distributed along the longitudinal and vertical gradients in winter. Summer surface stratification of CO₂ developed at a depth of 5 m from approximately 350 km river reach and gradually extended to the dam site, which corresponded well to a weak thermal stratification in the summer season.

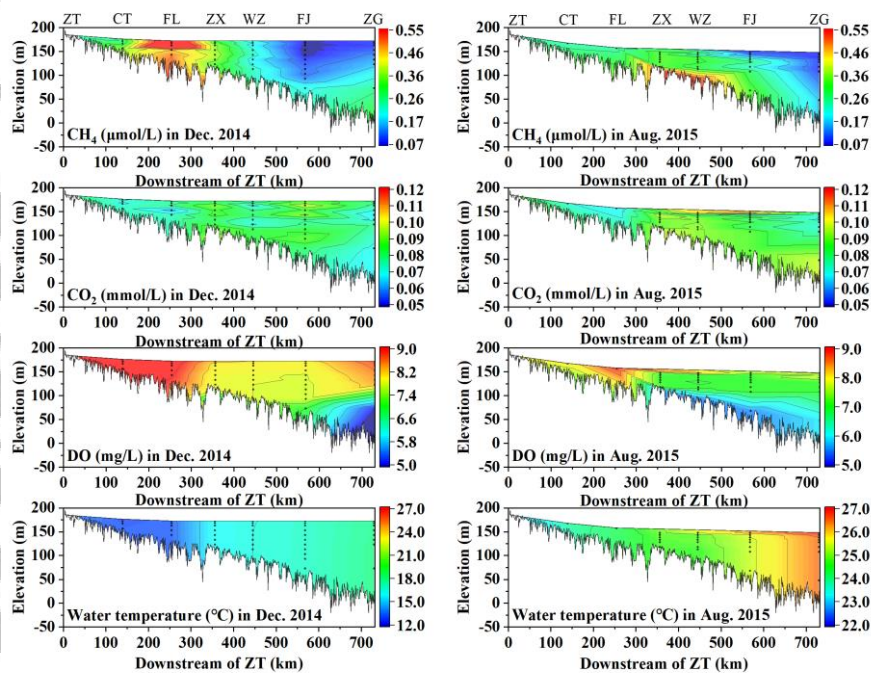


Figure 5 Profiles of CO₂, CH₄, dissolved oxygen (DO) and water temperature along the main stem of the Yangtze in Three Gorges Reservoir. Small dots along a vertical line in the profiles indicate the sampling locations.

3.4 Relationship between CH₄ and sediments in water column

In summer, the sedimentation rate of TPM, POM, POC and PP showed significant positive correlations with CH₄ concentrations in the TGR (Spearman correlation, $r_{\text{CH}_4\text{-TPM-summer}} = 0.60$; $r_{\text{CH}_4\text{-POM-summer}} = 0.56$; $r_{\text{CH}_4\text{-POC-summer}} = 0.62$; $r_{\text{CH}_4\text{-PP-summer}} = 0.59$, $p < 0.05$). To predict CH₄ concentration in the water column, linear regression model between CH₄ concentrations and the sedimentation rate of the above variables in summer were shown in Figure 6. The linear regression model of PON and CH₄ in summer did not pass the significant test ($p \geq 0.05$). The

statistical correlations between sediments and CH₄ concentrations were much weaker or even statistically insignificant in winter. Thus, we did not proceed linear regression models based on winter datasets to predict CH₄ concentrations.

With respect to the stoichiometry of sediments in summer, there were significant negative correlations between CH₄ concentrations and particulate C/P ratio and there were positive correlations between CH₄ levels and particulate C/N ratios (Spearman correlation, $r_{\text{CH}_4\text{-POC/PP-summer}} = -0.81$; $r_{\text{CH}_4\text{-POC/PON-summer}} = 0.63$, $p < 0.05$). These two correlations were more significant in the larger sediments, e.g., $>50 \mu\text{m}$ and $30 \sim 50 \mu\text{m}$, whereas the smaller sediments did not show evident statistical correlations. As such, linear regression models, i.e. between CH₄ concentrations and stoichiometry of sediments, were shown in Figure 7A and 7B. There was no clear evidence showing a contribution of POC/PON to CH₄ in winter (data not shown). Yet, the change of $\delta^{13}\text{C-POC}$ in suspended sediments in winter significantly impacted the concentrations of CH₄ and CO₂. Linear regression models between them were shown in Figure 7C and 7D.

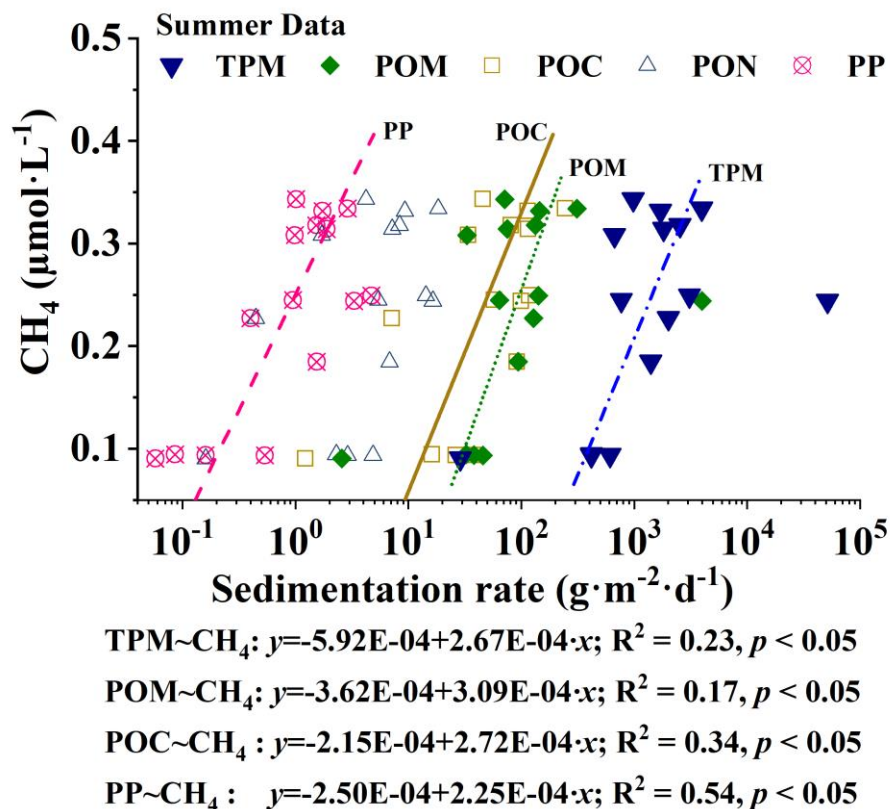


Figure 6. Scatter plots of CH₄ and sedimentation rates of C, N and P in summer. Linear regression results in the figure passed significance test ($p < 0.05$)

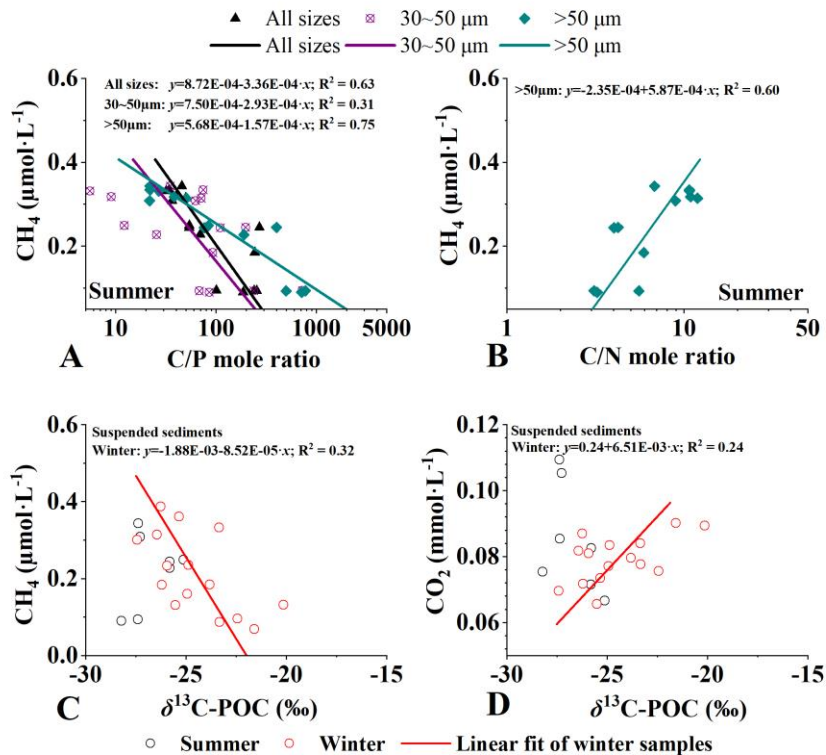


Figure 7. Scatter plots of CH₄ with particulate C/P ratio (A) and C/N ratio (B), and scatter plots of CO₂, CH₄ with δ¹³C-POC (C) and (D). Linear regression results in the figure passed significance test ($p < 0.05$)

3.5 Modeling of reservoir sedimentation of POC, PON and PP

Reservoir sedimentation of C, N and P exhibited large spatial variations along the river-reservoir gradient and varied with the time of reservoir age. The mid part of the TGR, (the dark gray zone in the Figure 8), accumulated the largest amounts of sediment of all size ranges in all years. Most POC, PON and PP were settled and accumulated in the mid-part of the reservoir. Large size POC and PON (> 50 μm), were in general among the earliest settled in the upper part of the reservoir. However, the smallest size of PP (< 10 μm) were the earliest to settle in the upper reservoir. Smaller sizes of POC and PON were transported further downstream. With the increase in reservoir age, reservoir sedimentation of C, N and P tended to accumulate downstream. However, the narrow gorges reach in the TGR at 600-700 km downstream of ZT limited reservoir sedimentation resulting in the "lag" curve at this part.

Differences in sedimentation rates of POC, PON and PP resulted in distinctive stoichiometric patterns in reservoir sediments. Particulate C/N ratios for different size ranges were all above the Redfield ratio (the dash-dot line in Figure 8). Distinctive variations of POC/PON ratio were apparent among different size ranges. The stoichiometric patterns of particulate C/P ratios and N/P ratios were similar. The smallest size (<10 μm) sediments showed a significant increase towards downstream. They were below the Redfield ratio at the upper part of the TGR and passed through the Redfield ratio at the middle part of the TGR. Our field observations of POC/PP showed the similar trend (Supporting information S5).

With the increase in years of reservoir operation, the particulate C/P and N/P ratios increased in the lower part of the TGR, however, at the upper and mid part of the TGR, these differences were not evident.

Long-term model simulation (Figure 8) increased our understanding of the imbalance stoichiometric sedimentation in the TGR. Averaged particulate C:N:P proportions in the sediment layer along the upper, mid and lower part of the TGR in the first 30 years of reservoir operation were estimated to be 68:7:1, 97:8:1, 151:13:1. Mid-part of the TGR has the stoichiometry near the Redfield ratio. In addition, a holistic estimate of particulate C:N:P in the sediment layer of the TGR was 100:8:1, implying that apparently more C than N would accumulated and retained by the TGR compared to the above global estimates. P, specifically in smaller size particles (<10 μm), seemed to be the potential key driver that regulates particulate C:N:P in the sediment layer of the TGR [Zhou *et al.*, 2015]. Its sedimentation, primarily in the mid part of the TGR, contributed to the significant decreases in particulate C/P and N/P ratios, and could support long-term CH_4 production in the reservoir.

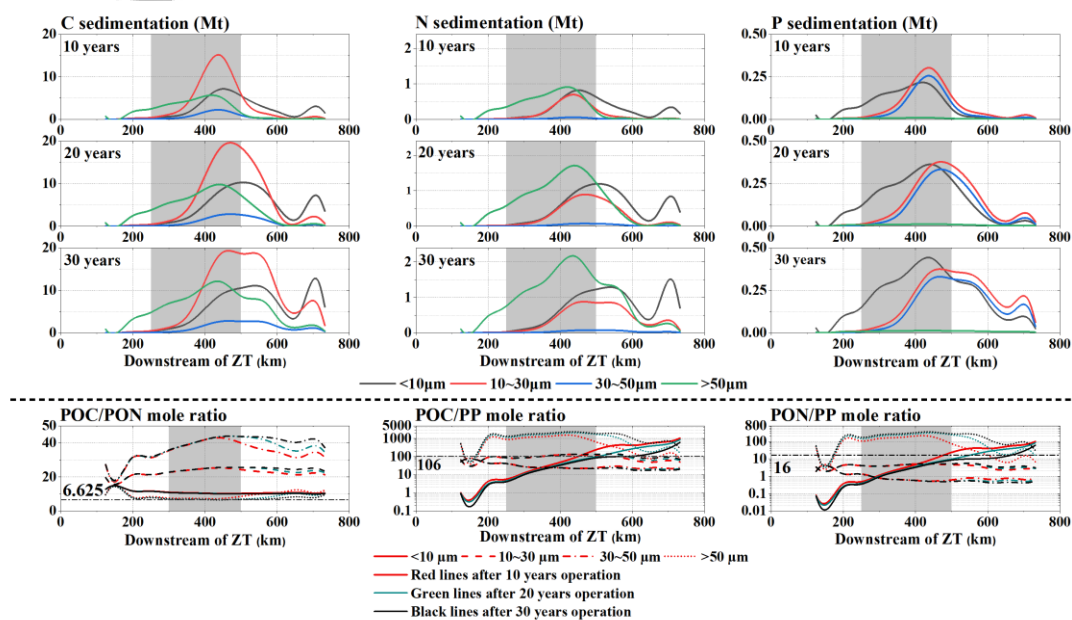


Figure 8. Predictions of POC, PON and PP sedimentation and their stoichiometry along the longitudinal direction of the Yangtze main stem in the TGR. Dark gray areas indicate the mid part of the TGR.

4 Discussion

4.1 Large amount of sediments deposited in the mid-part of the reservoir.

One of the important conceptual models in reservoir limnology is that reservoir hydrodynamic characteristics structure longitudinal gradients in its ecosystem parameters,

such as light availability, origin and transport of macronutrients, primary production and development of food webs [Straškraba, 1999; Thornton *et al.*, 1990].

The TGR is a river-valley dammed reservoir. Over 60% of inflow water and nearly 70% of sediments are from upstream of Yangtze main stem (Figure 1). Together with the two large tributaries, i.e. the Jialing and Wu River (Figure 1), over 80% of inflow and sediments are input from upper part of the TGR [Huang *et al.*, 2019; W Li *et al.*, 2018]. Particularly, the summer flood season (June to September) received over 80% of annual sediments from upstream. Longitudinal decrease of water velocity and increase of water retention time in such hydro-morphological characteristics cause the large deposition of input sediments (or TPM) in the mid part of the reservoir, particular from FL to ZX [Huang *et al.*, 2019; W Li *et al.*, 2018]. Both of our field observations and modeling work evidently supported the above inference.

4.2 Imbalanced stoichiometric sedimentation caused by hydrodynamic gradients.

Suspended sediments from upstream river basin were likely a mixture of minerals, e.g., gravels, sands, silts, muds, and aggregates of various organic materials (including soil organic matter, leaves and needles, macrophytes, woody debris, other plant parts, detritus from plankton and other aquatic organisms) [Allan and Castillo, 2007; Wetzel, 2001]. The various types of particulates in suspended sediments have different densities and stoichiometry of C, N and P. In general, particulate C and N exist mainly in organic forms. Comparatively, P have large potential for absorption of heavier inorganic minerals in the TGR, particularly smaller sized ($< 10 \mu\text{m}$) sediments [Meng *et al.*, 2014; Tang *et al.*, 2018; Zhang *et al.*, 2012]. Thus, PP is evidently heavier than POC and PON and seemed to be likely among the first to "lost" in water column via sedimentation from upstream of the TGR towards downstream.

Such potent sedimentation of PP in the upper and mid part of the TGR regulated imbalanced stoichiometry of trapped sediments from a lower range than the Redfield ratio to a higher range in the mid-part of the reservoir, particularly the small size from the modeling results. Trapped sediments, particularly in summer, exhibited a longitudinal increase of particulate C/P ratio in such lotic to lentic hydrodynamic gradients. Thus, it seemed to be plausible that P limitation for microorganisms would becoming prevailing in the lower part of the TGR.

POM with higher C/N ratio and $\delta^{13}\text{C}$ -POC values mostly originated from terrestrial sources, being less degradable and isotopically heavier than aquatic autochthonous POM [Allan and Castillo, 2007; Kendall *et al.*, 2001]. When entering into the TGR, terrestrial coarse POM input from upstream might be broken down or decomposed by turbulence and shear stress. Smaller size POM (POC and PON) in trapped sediments were lighter and could be transported further downstream. The mid-part of the reservoir exhibited an evident shift of sources of POM in both stoichiometry and its stable isotopic ratios. With the gradual increase of autochthonous OM (Figure 4), we believed that POM would gradually become more biodegradable in mid-part of the reservoir, supporting fast fermentation of OC for methane production [Grasset *et al.*, 2018].

4.3 CH₄ accumulation strongly depended on the sedimentation of PP and POM

Compared with global datasets synthesized by Stanley *et al.* [2016], the concentration level of CH₄ in the TGR (CH₄ Range: $0.069\mu\text{mol/L} \sim 0.694\mu\text{mol/L}$) approximately covered the range of the 1st and 3rd quantiles of the global datasets by Stanley *et al.* [2016], i.e. CH₄ Range: $0.098\mu\text{mol/L} \sim 0.612\mu\text{mol/L}$. The well-mixed hydrodynamic condition limited formation of strong and persistent hypoxia or anoxia in water column at the main stem of the

TGR. Thermal stratification in summer was also restricted in main stem (Figure 5). These characteristics support our inference that the TGR was not a productive system of CH₄ compared to tropical reservoirs [Adams, 2005; Robert Delmas *et al.*, 2005]. Thus, external OM supply from sediment processes evidently supports the CH₄ accumulation. Increased allochthonous OM input from upstream and settled in the mid-part of the reservoir fueled CH₄ accumulation here.

Although the biological mechanisms of methanogenesis and methanotrophs have been widely studied, little is known to date about how the stoichiometry of C, N and P modulate methanogenesis and methanotrophs. A recent study by Kim *et al.* [2015] showed that methanogenesis seemed to be stimulated solely by P addition, whereas N addition may inhibit microbial activity or switches the direction of OC fermentation. Thus, the contribution of P sedimentation to CH₄ accumulation in the TGR seemed to be plausible from our field observations. It was not only because the sedimentation of P and POM co-occurred in the mid-part of the reservoir. More P relative to C seemed to be favor by CH₄ accumulation in the TGR (Figure 7), implying that P may stimulate or modulate to CH₄ production in the mid part of the reservoir [Kim *et al.*, 2015].

4.4 Uncertainties and limitations

The overall sedimentation rate was likely low in winter. While the concentration of particulate P is low in water column, it was below the detection limit in trapped sediments, and could not support our analysis about the imbalanced stoichiometric sedimentation. From our field data, e.g. stable isotope values (Figure 4), it seemed that OM in winter were "homogenized" caused by the switch of hydrodynamic condition to lentic type in the TGR (Figure 1). Dissolved organic carbon (DOC) and nutrients in the TGR may be also important in winter to contribute CH₄ production. Yet, more data is needed.

CH₄ in the water column is the balance between both methanogenesis, mostly in strictly anaerobic sediment layers, and methanotrophs, primarily occurring in oxic sediment or water columns [Stanley *et al.*, 2016]. Methanogenesis can account for over 50% of the total carbon mineralization in lake sediments [Donis *et al.*, 2017; Rodriguez *et al.*, 2018]. Methane oxidation can be comparable to total heterotrophic bacterial production, or in some lakes can even represent primary production, and results in substantial formations of microbial biomass [Bastviken, 2009; Bürgmann, 2011; Morana *et al.*, 2015]. Although we tried to elaborate our observations from the aspect of methanogenesis in the TGR, to the limit of our study, we did not directly measure methane production rates on site. It also seemed to be evident that methanotrophs in oxic sediment layers or water column would be regulated by P [Ho *et al.*, 2013; Veraart *et al.*, 2015; Yu *et al.*, 2017]. Thus, the rates of methanogenesis and methanotrophs in the TGR are needed for further study to provide direct evidences.

5 Conclusions

A majority of sediments settled in the mid-part of the TGR, particularly in the summer season. Hydrodynamic gradients in the river-valley dammed reservoir structured imbalanced stoichiometric sedimentation. The mid-part of the TGR, being the "hot spot" of methane accumulation, exhibited an evident shift of sources of POM in both stoichiometry and its stable isotopic ratios. It seemed to be plausible that continuous sedimentation of P in the mid part of the TGR potentially regulated the imbalanced stoichiometry of sediments and may contribute to the long-term methane production here.

Acknowledgments, Samples, and Data

The National Natural Science Foundation of China (Project No. 51861125204, and 51679226) supported this work. Dr. Zhe Li is also supported by the “Chongqing Talent” Program funded by the government of Chongqing Municipality. We thank the China Three Gorges Corporation for providing partial funding support for monthly sampling and daily hydrological data of the Three Gorges Reservoir. Special thanks to Dr. Man Zhang, and Prof. Jianjun Zhou from Tsinghua University who provided updated modeling results based on Zhou *et al.* [2015]. We also thank Mr. Xiao Yao, Mr. Zhikun Yin, and Mr. Hailong Du who participated in the field sampling campaign.

Original field data have been uploaded on HydroShare:

Li, Z., L. Lu, P. Lv, Z. Zhang, J. Guo (2020). Imbalanced stoichiometric reservoir sedimentation fuels methane emissions in China's Three Gorges Reservoir, HydroShare, <http://www.hydroshare.org/resource/37b858a52d81477db9f177c55b644e03>

References

- Aben, R. C. H., et al. (2017), Cross continental increase in methane ebullition under climate change, *Nature Communications*, 8.
- Abril, G., F. Guerin, S. Richard, R. Delmas, C. Galy-Lacaux, P. Gosse, A. Tremblay, L. Varfalvy, M. A. dos Santos, and B. Matvienko (2005), Carbon dioxide and methane emissions and the carbon budget of a 10-year old tropical reservoir (Petit Saut, French Guiana), *Global Biogeochemical Cycles*, 19(4).
- Adams, D. D. (2005), Diffuse Flux of Greenhouse Gases — Methane and Carbon Dioxide — at the Sediment-Water Interface of Some Lakes and Reservoirs of the World, in *Greenhouse Gas Emissions — Fluxes and Processes: Hydroelectric Reservoirs and Natural Environments*, edited by A. Tremblay, L. Varfalvy, C. Roehm and M. Garneau, pp. 129-153, Springer Berlin Heidelberg, Berlin, Heidelberg.
- Allan, J. D., and M. M. Castillo (2007), *Stream Ecology: Structure and function of running waters*, XIV, 436 pp., Springer Netherlands, Netherlands.
- APHA, AWWA, and WEF (2005), *Standard Methods for the Examination of Water & Wastewater*, American Public Health Association.
- Baker, J. E., S. J. Eisenreich, and B. J. Eadie (1991), Sediment trap fluxes and benthic recycling of organic carbon, polycyclic aromatic hydrocarbons, and polychlorobiphenyl congeners in Lake Superior, *Environmental Science & Technology*, 25(3), 500-509.
- Barros, N., J. J. Cole, L. J. Tranvik, Y. T. Prairie, D. Bastviken, V. L. M. Huszar, P. del Giorgio, and F. Roland (2011), Carbon emission from hydroelectric reservoirs linked to reservoir age and latitude, *Nature Geoscience*, 4(9), 593-596.
- Bastviken, D. (2009), Methane, in *Encyclopedia of Inland Waters*, edited by G. E. Likens, pp. 783-805, Academic Press, Oxford.
- Bernhardt, E. S., J. R. Blaszczak, C. D. Ficken, M. L. Fork, K. E. Kaiser, and E. C. Seybold (2017), Control Points in Ecosystems: Moving Beyond the Hot Spot Hot Moment Concept, *Ecosystems*, 20(4), 665-682.
- Bürgmann, H. (2011), Methane Oxidation (Aerobic), in *Encyclopedia of Geobiology*, edited by J. Reitner and V. Thiel, pp. 575-578, Springer Netherlands, Dordrecht.
- Clow, D. W., S. M. Stackpoole, K. L. Verdin, D. E. Butman, Z. L. Zhu, D. P. Krabbenhoft, and R. G. Striegl (2015), Organic Carbon Burial in Lakes and Reservoirs of the Conterminous United States, *Environmental Science & Technology*, 49(13), 7614-7622.
- Cole, J. J., et al. (2007), Plumbing the global carbon cycle: Integrating inland waters into the terrestrial carbon budget, *Ecosystems*, 10, 171-184.
- Deemer, B. R., J. A. Harrison, S. Li, J. J. Beaulieu, T. Delsontro, N. Barros, J. F. Bezerra-Neto, S. M. Powers, M. A. dos Santos, and J. A. Vonk (2016), Greenhouse Gas Emissions from Reservoir Water Surfaces: A New Global Synthesis, *Bioscience*, 66(11), 949-964.
- Delmas, R., C. Galy-Lacaux, and S. Richard (2001), Emissions of greenhouse gases from the tropical hydroelectric reservoir of Petit Saut (French Guiana) compared with emissions from thermal alternatives, *Global Biogeochemical Cycles*, 15(4), 993-1003.
- Delmas, R., S. Richard, F. Guérin, G. Abril, C. Galy-Lacaux, C. Delon, and A. Grégoire (2005), Long Term Greenhouse Gas Emissions from the Hydroelectric Reservoir of Petit Saut (French Guiana) and Potential Impacts, in *Greenhouse Gas Emissions — Fluxes and Processes: Hydroelectric Reservoirs and Natural*

Environments, edited by A. Tremblay, L. Varfalvy, C. Roehm and M. Garneau, pp. 293-312, Springer Berlin Heidelberg, Berlin, Heidelberg.

DelSontro, T., D. F. McGinnis, B. Wehrli, and I. Ostrovsky (2015), Size Does Matter: Importance of Large Bubbles and Small-Scale Hot Spots for Methane Transport, *Environmental Science & Technology*, 49(3), 1268-1276.

Donis, D., S. Flury, A. Stöckli, J. E. Spangenberg, D. Vachon, and D. F. McGinnis (2017), Full-scale evaluation of methane production under oxic conditions in a mesotrophic lake, *Nature Communications*, 8(1), 1661.

Goldenfum, J. A. (2010), GHG measurement guidelines for freshwater reservoir, 1-138 pp, The UNESCO/IHA Greenhouse Gas Emission from Freshwater Reservoirs Research Project, UK.

Grantz, E. M., B. E. Haggard, and J. T. Scott (2014), Stoichiometric imbalance in rates of nitrogen and phosphorus retention, storage, and recycling can perpetuate nitrogen deficiency in highly-productive reservoirs, *Limnology and Oceanography*, 59(6), 2203-2216.

Grasset, C., R. Mendonca, G. V. Saucedo, D. Bastviken, F. Roland, and S. Sobek (2018), Large but variable methane production in anoxic freshwater sediment upon addition of allochthonous and autochthonous organic matter, *Limnology and Oceanography*, 63(4), 1488-1501.

Hamilton-taylor, J., M. Willis, and C. S. Reynolds (1984), Depositional fluxes of metals and phytoplankton in Windermere as measured by sediment traps, *Limnology and Oceanography*, 29(4), 695-710.

Hertwich, E. G. (2013), Addressing Biogenic Greenhouse Gas Emissions from Hydropower in LCA, *Environmental Science & Technology*, 47(17), 9604-9611.

Ho, A., F.-M. Kerckhof, C. Luke, A. Reim, S. Krause, N. Boon, and P. L. E. Bodelier (2013), Conceptualizing functional traits and ecological characteristics of methane-oxidizing bacteria as life strategies, *Environmental Microbiology Reports*, 5(3), 335-345.

Huang, Y., J. Wang, and M. Yang (2019), Unexpected sedimentation patterns upstream and downstream of the Three Gorges Reservoir: Future risks, *International Journal of Sediment Research*, 34(2), 108-117.

Kendall, C., S. R. Silva, and V. J. Kelly (2001), Carbon and nitrogen isotopic compositions of particulate organic matter in four large river systems across the United States, *Hydrological Processes*, 15(7), 1301-1346.

Kim, S. Y., A. J. Veraart, M. Meima-Franke, and P. L. E. Bodelier (2015), Combined effects of carbon, nitrogen and phosphorus on CH₄ production and denitrification in wetland sediments, *Geoderma*, 259-260, 354-361.

Li, W., S. Yang, Y. Xiao, X. Fu, J. Hu, and T. Wang (2018), Rate and Distribution of Sedimentation in the Three Gorges Reservoir, Upper Yangtze River, *Journal of Hydraulic Engineering*, 144(8), 05018006.

Li, Z., H. Du, Y. Xiao, and J. Guo (2017a), Carbon footprints of two large hydro-projects in China: Life-cycle assessment according to ISO/TS 14067, *Renewable Energy*, 114, 534-546.

Li, Z., L. Lu, J. Guo, J. Yang, J. Zhang, B. He, and L. Xu (2017b), Responses of spatial-temporal dynamics of bacterioplankton community to large-scale reservoir operation: a case study in the Three Gorges Reservoir, China, *Scientific Reports*, 7, 42469.

Maeck, A., H. Hofmann, and A. Lorke (2014), Pumping methane out of aquatic sediments - ebullition forcing mechanisms in an impounded river, *Biogeosciences*, 11(11), 2925-2938.

Maeck, A., T. DelSontro, D. F. McGinnis, H. Fischer, S. Flury, M. Schmidt, P. Fietzek, and A. Lorke (2013), Sediment Trapping by Dams Creates Methane Emission Hot Spots, *Environmental Science & Technology*, 47(15), 8130-8137.

McGinnis, D. F., J. Greinert, Y. Artemov, S. E. Beaubien, and A. Wuest (2006), Fate of rising methane bubbles in stratified waters: How much methane reaches the atmosphere?, *J. Geophys. Res.*, 111(C9), 1.

Mendonca, R., S. Kosten, S. Sobek, S. J. Cardoso, M. P. Figueiredo-Barros, C. H. Duque Estrada, and F. Roland (2016), Organic carbon burial efficiency in a subtropical hydroelectric reservoir, *Biogeosciences*, 13(11), 3331-3342.

Meng, J., Q. Yao, and Z. Yu (2014), Particulate phosphorus speciation and phosphate adsorption characteristics associated with sediment grain size, *Ecological Engineering*, 70, 140-145.

Meyers, P. A., M. J. Leenheer, B. J. Eadie, and S. J. Maule (1984), Organic geochemistry of suspended and settling particulate matter in Lake Michigan, *Geochimica Et Cosmochimica Acta*, 48(3), 443-452.

Morana, C., A. V. Borges, F. A. E. Roland, F. Darchambeau, J. P. Descy, and S. Bouillon (2015), Methanotrophy within the water column of a large meromictic tropical lake (Lake Kivu, East Africa), *Biogeosciences*, 12(7), 2077-2088.

Parnell, A., R. Inger, S. Bearhop, and A. Jackson (2008), SIAR: stable isotope analysis in R, *R package version*, 3.

Parnell, A. C., R. Inger, S. Bearhop, and A. L. Jackson (2010), Source partitioning using stable isotopes: coping with too much variation, *PloS one*, 5(3), e9672.

Peeters, F., J. E. Fernandez, and H. Hofmann (2019), Sediment fluxes rather than oxic methanogenesis explain diffusive CH₄ emissions from lakes and reservoirs, *Scientific Reports*, 9.

Powers, S. M., J. P. Julian, M. W. Doyle, and E. H. Stanley (2013), Retention and transport of nutrients in a mature agricultural impoundment, *Journal of Geophysical Research: Biogeosciences*, 118(1), 91-103.

- Prairie, Y., et al. (2018), Greenhouse Gas Emissions from Freshwater Reservoirs: What Does the Atmosphere See?, *Ecosystems*, 21(5), 1058-1071.
- Redfield, A. C. (1960), The biological control of chemical factors in the environment, *Science Progress*, 11(11), 150-170.
- Rodriguez, M., T. Gonsiorczyk, and P. Casper (2018), Methane production increases with warming and carbon additions to incubated sediments from a semiarid reservoir, *Inland Waters*, 8(1), 109-121.
- Sobek, S., T. DelSontro, N. Wongfun, and B. Wehrli (2012), Extreme organic carbon burial fuels intense methane bubbling in a temperate reservoir, *Geophysical Research Letters*, 39.
- Sollberger, S., B. Wehrli, C. J. Schubert, T. DelSontro, and W. Eugster (2017), Minor methane emissions from an Alpine hydropower reservoir based on monitoring of diel and seasonal variability, *Environmental Science-Processes & Impacts*, 19(10), 1278-1291.
- Stanley, E. H., N. J. Casson, S. T. Christel, J. T. Crawford, L. C. Loken, and S. K. Oliver (2016), The ecology of methane in streams and rivers: patterns, controls, and global significance, *Ecological Monographs*, 86(2), 146-171.
- Straškraba, M. (1999), Retention time as a key variable of reservoir limnology, *Theoretical reservoir ecology and its applications. São Carlos: International Institute of Ecology, Brazilian Academy of Sciences and Backhuys Publishers*, 385-410.
- Tang, X., M. Wu, and R. Li (2018), Phosphorus distribution and bioavailability dynamics in the mainstream water and surface sediment of the Three Gorges Reservoir between 2003 and 2010, *Water Research*, 145, 321-331.
- Team, R. C. (2020), R: A language and environment for statistical computing., edited, R Foundation for Statistical Computing, Vienna, Austria.
- Thornton, K. W., B. L. Kimmel, and F. E. Payne (1990), *Reservoir limnology: ecological perspectives*, John Wiley & Sons.
- Tranvik, L. J., et al. (2009), Lakes and reservoirs as regulators of carbon cycling and climate, *Limnology and Oceanography*, 54(6), 2298-2314.
- Veraart, A. J., A. K. Steenbergh, A. Ho, S. Y. Kim, and P. L. E. Bodelier (2015), Beyond nitrogen: The importance of phosphorus for CH₄ oxidation in soils and sediments, *Geoderma*, 259, 337-346.
- Walter, K. M., J. P. Chanton, F. S. Chapin, E. A. G. Schuur, and S. A. Zimov (2008), Methane production and bubble emissions from arctic lakes: Isotopic implications for source pathways and ages, *J. Geophys. Res.*, 113, 1.
- Wang, J., B. Gu, J. Huang, X. Han, G. Lin, F. Zheng, and Y. Li (2014), Terrestrial contributions to the aquatic food web in the middle Yangtze River, *PLoS One*, 9(7), e102473.
- Wetzel, R. G. (2001), *Limnology: Lake and River Ecosystems*, Academic Press, San Diego.
- Wilkinson, J., P. Bodmer, and A. Lorke (2019), Methane dynamics and thermal response in impoundments of the Rhine River, Germany, *Science of The Total Environment*, 659, 1045-1057.
- Williamson, C. E., J. E. Saros, W. F. Vincent, and J. P. Smol (2009), Lakes and reservoirs as sentinels, integrators, and regulators of climate change, *Limnology and Oceanography*, 54(6), 2273-2282.
- Wu, Y., J. Zhang, S. M. Liu, Z. F. Zhang, Q. Z. Yao, G. H. Hong, and L. Cooper (2007), Sources and distribution of carbon within the Yangtze River system, *Estuarine, Coastal and Shelf Science*, 71(1-2), 13-25.
- Xiang, Z. A. (2000), Review on river sediment size analyses, in *Anthology of River Sediment Measurements [in Chinese]*, edited by C. Bureau of Hydrology, pp. 226-245, Huanghe Water Conservancy Press, Zhengzhou, China.
- Xiao, Y., Z. Li, J. Guo, F. Fang, and V. H. Smith (2016), Succession of phytoplankton assemblages in response to large-scale reservoir operation: a case study in a tributary of the Three Gorges Reservoir, China, *Environmental Monitoring and Assessment*, 188(3).
- Yu, L., Y. Wang, X. Zhang, P. Dorsch, and J. Mulder (2017), Phosphorus addition mitigates N₂O and CH₄ emissions in N-saturated subtropical forest, SW China, *Biogeosciences*, 14(12), 3097-3109.
- Zhang, B., F. Fang, J. S. Guo, Y. P. Chen, Z. Li, and S. S. Guo (2012), Phosphorus fractions and phosphate sorption-release characteristics relevant to the soil composition of water-level-fluctuating zone of Three Gorges Reservoir, *Ecological Engineering*, 40, 153-159.
- Zhou, J., and B. Lin (1998), One-Dimensional Mathematical Model for Suspended Sediment by Lateral Integration, *Journal of Hydraulic Engineering*, 124(7), 712-717.
- Zhou, J., M. Zhang, B. Lin, and P. Lu (2015), Lowland fluvial phosphorus altered by dams, *Water Resources Research*, 51(4), 2211-2226.